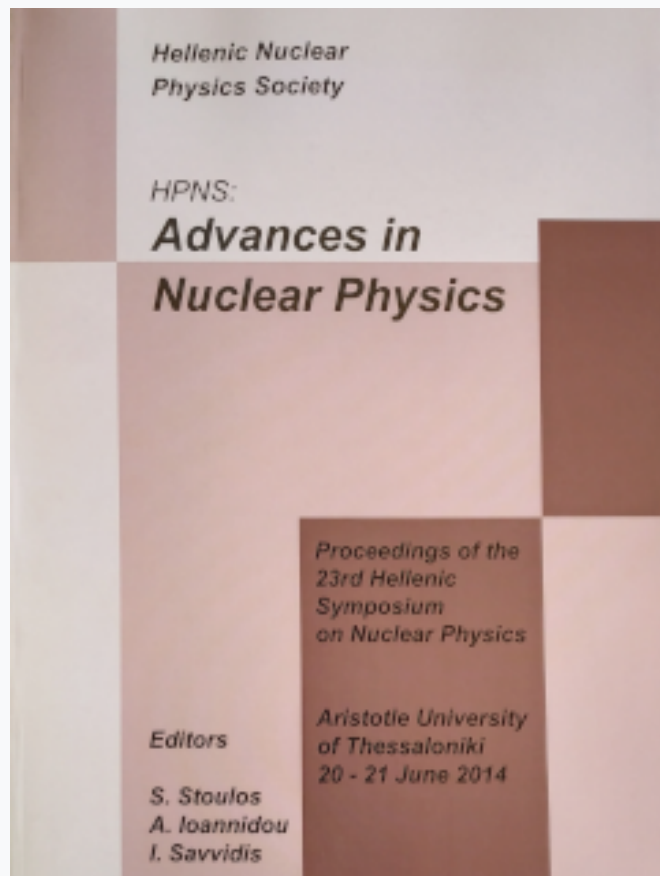


## HNPS Advances in Nuclear Physics

Vol 22 (2014)

HNPS2014



### Measurement of the $^{242}\text{Pu}(\text{n},\text{f})$ cross-section at the CERN n\_TOF facility

A. Tsinganis, E Berthoumieux, C. Guerrero, N. Colonna, M. Calviani, R. Vlastou, S. Andriamonje, V. Vlachoudis, F. Gunsing, C. Massimi, the *n\_TOF* Collaboration

doi: [10.12681/hnps.1926](https://doi.org/10.12681/hnps.1926)

### To cite this article:

Tsinganis, A., Berthoumieux, E., Guerrero, C., Colonna, N., Calviani, M., Vlastou, R., Andriamonje, S., Vlachoudis, V., Gunsing, F., Massimi, C., & *n\_TOF* Collaboration, the. (2019). Measurement of the  $^{242}\text{Pu}(\text{n},\text{f})$  cross-section at the CERN *n\_TOF* facility. *HNPS Advances in Nuclear Physics*, 22, 28–33. <https://doi.org/10.12681/hnps.1926>

# Measurement of the $^{242}\text{Pu}(\text{n},\text{f})$ cross-section at the CERN n\_TOF facility \*

A. Tsinganis<sup>1,2</sup>, E. Berthoumieux<sup>3</sup>, C. Guerrero<sup>2</sup>, N. Colonna<sup>4</sup>, M. Calviani<sup>2</sup>, R. Vlastou<sup>1</sup>, S. Andriamonje<sup>2</sup>, V. Vlachoudis<sup>2</sup>, F. Gunsing<sup>3</sup>, C. Massimi<sup>5</sup>, and the n\_TOF Collaboration<sup>6</sup>

<sup>1</sup> National Technical University of Athens (NTUA), Greece

<sup>2</sup> European Organisation for Nuclear Research (CERN), Geneva, Switzerland

<sup>3</sup> Commissariat a l'Energie Atomique (CEA) Saclay - Irfu, Gif-sur-Yvette, France

<sup>4</sup> Istituto Nazionale di Fisica Nucleare, Bari, Italy

<sup>5</sup> Dipartimento di Fisica e Astronomia, Università di Bologna, and Sezione INFN di Bologna, Italy

<sup>6</sup> [www.cern.ch/ntof](http://www.cern.ch/ntof)

---

## Abstract

Knowledge of neutron cross-sections of various plutonium isotopes and other minor actinides is crucial for the design of advanced nuclear systems. The  $^{240,242}\text{Pu}(\text{n},\text{f})$  cross-sections were measured at the CERN n\_TOF facility, taking advantage of the wide energy range (from thermal to GeV) and the high instantaneous flux of the neutron beam. In this work, preliminary results are presented along with a theoretical cross-section calculation performed with the EMPIRE code.

---

## INTRODUCTION

The accurate knowledge of neutron cross-sections of a variety of plutonium isotopes and other minor actinides is crucial for feasibility and performance studies of advanced nuclear systems. In particular, the non-fissile and long-lived  $^{240,242}\text{Pu}$  isotopes contribute to the long-term residual activity of nuclear waste and the  $^{240,242}\text{Pu}(\text{n},\text{f})$  cross-sections are included in the NEA High-Priority List [1]. In this context, the  $^{240,242}\text{Pu}(\text{n},\text{f})$  cross-section was measured at the CERN n\_TOF facility [2-4] relative to the well-known  $^{235}\text{U}(\text{n},\text{f})$  cross-section. Preliminary results are presented in this work.

## 1. EXPERIMENTAL SETUP

### 1.1 The n\_TOF facility

At n\_TOF, neutrons are produced through spallation induced by a 20 GeV/c bunched proton beam impinging on a massive lead target and subsequent moderation in a few centimetres thick layer of (borated) water. The produced neutrons have energies starting from thermal and up to over 10 GeV and travel along an approximately 185 m long path to reach the experimental area. This allows covering the region of interest in a single experiment, thus reducing uncertainties related to different measurements performed in separate neutron energy ranges. The high instantaneous flux of the n\_TOF neutron beam mitigates the adverse effects of the strong  $\alpha$ -particle background produced by the samples and the low fission cross-section below and near the fission threshold.

### 1.2 Samples

Eight plutonium oxide ( $\text{PuO}_2$ ) samples manufactured at IRMM, Geel, were used [5] ( $4 \times ^{240}\text{PuO}_2$ ,  $4 \times ^{242}\text{PuO}_2$ ), for a total mass of 3.1 mg of  $^{240}\text{Pu}$  ( $\sim 0.11 \text{ mg/cm}^2$  per sample, 99.90% purity) and 3.6 mg of  $^{242}\text{Pu}$  ( $\sim 0.13 \text{ mg/cm}^2$  per sample, 99.97% purity). The material was electro-deposited on aluminium backing 0.25 mm thick and 5 cm in diameter; while the deposit itself had a diameter of 3 cm. Various contaminants were present, mainly in the form of other plutonium isotopes, such as  $^{238}\text{Pu}$ ,  $^{239}\text{Pu}$ ,  $^{241}\text{Pu}$  and

$^{244}\text{Pu}$ . While these impurities are present in very small amounts, the high fission cross-sections of fissile contaminants compared to the isotopes of interest dominate in parts of the energy range studied. Additionally, a  $^{235}\text{U}$  sample ( $\text{UF}_4$ ) with a mass of 18 mg deposited on a 0.2 mm thick aluminium backing was used as reference. Since this sample had a diameter of 7 cm, its active area was reduced with a thin aluminium mask to match the diameter of the plutonium samples. The active mass was therefore reduced to 3.3 mg of  $^{235}\text{U}$  ( $\sim 0.47 \text{ mg/cm}^2$ ).

### 1.3 Detectors and data acquisition

The measurements were carried out with Micromegas (Micro-MEsh GAsous Structure) gas detectors [6]. The gas volume of the Micromegas is separated into a charge collection region (several mm) and an amplification region (typically tens of  $\mu\text{m}$ ) by a thin “micromesh” with 35  $\mu\text{m}$  diameter holes on its surface. The amplification that takes place in the amplification region significantly improves the signal-to-noise ratio of the detector. This is of special importance for the high neutron energy region, where the fission signals are recorded within a few  $\mu\text{s}$  of the  $\gamma$ -flash (see section 2.2). The chamber housing the samples and detectors was filled with an  $\text{Ar:CF}_4:\text{isoC}_4\text{H}_{10}$  gas mixture (88:10:2) at a pressure of 1 bar and under constant circulation.

Existing electronics from previous fission measurements were used for signal shaping. Additional electronic protection was added to the pre-amplifier channels to prevent breakage, while the mesh voltage value was chosen to minimize the number of sparks and subsequent trips. Furthermore, the shielding of the pre-amplifier module was improved to mitigate the baseline oscillation observed following the prompt  $\gamma$ -flash. The standard n\_TOF Data Acquisition System [2] based on 8-bit Acqiris flash-ADCs was used for recording and storing the raw data collected by the detectors at a sampling rate of 100 MHz.

Due to the low expected count rate for the measurement, the chamber was placed in the n\_TOF experimental area for several months and in parallel with other measurements performed at n\_TOF. Throughout the measurement, beam-off data were taken in order to record the  $\alpha$ - and spontaneous fission background produced by the samples.

### 1.4 Experimental issues

The analysis of the experimental data is complicated by certain features of the experimental setup and by sample-induced backgrounds. These include the baseline oscillation induced by the prompt “ $\gamma$ -flash” which is discussed in section 2.2 and the spontaneous fission background, particularly in  $^{242}\text{Pu}$ .

While the above factors can be dealt with, an unexpected effect of the high  $\alpha$ -activity of the samples ( $>6 \text{ MBq}$  for  $^{240}\text{Pu}$ ) was encountered in the course of the measurement, with a steady degradation of the fission fragment amplitude distribution. After the measurement, a visual inspection of the detectors used with the  $^{240}\text{Pu}$  samples revealed an obvious circular discolouration of the mesh whose dimension and position exactly matched those of the samples (Fig. 1, left panel). Upon closer inspection with a microscope (Fig. 1, right panel), it became clear that the micromesh had suffered serious mechanical damage, particularly around the rims of the holes which were evidently deformed.

The damage suffered by the detectors must lead to a deterioration of the electrical field and therefore of the detector gain and overall performance. Indeed, this was clearly observed in the  $^{240}\text{Pu}$  data, where fission fragment and  $\alpha$ -particle signals became virtually indistinguishable in the obtained pulse height spectra. Because of this, a considerable part of the  $^{240}\text{Pu}$  data must be discarded, partially compromising the measurement. Although there was no visible damage, a similar but less pronounced effect was observed in the  $^{242}\text{Pu}$  data, with a slow but non-negligible gain drift during the measurement. The data, therefore, were analysed in smaller subsets where the gain can be considered constant.

For the above reasons, results on  $^{242}\text{Pu}$  only are being presented in this article. Also based on these findings, a proposal [7] has been submitted and approved to measure the

$^{240}\text{Pu}(n,f)$  cross-section at n\_TOF's newly constructed Experimental Area II [8], where the higher neutron flux and improved background suppression (due to the shorter flight-path) will allow to perform the measurement in a much shorter time, thus avoiding the degradation of the detectors.

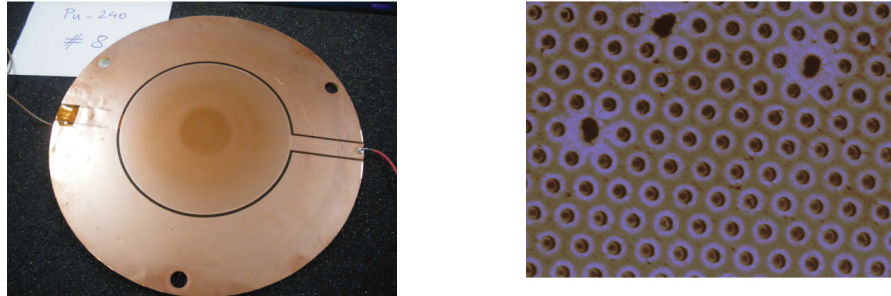


**Figure 1: Left:** One of the Micromegas detectors used with a  $^{240}\text{Pu}$  sample pictured after the end of the measurement. A 3 cm diameter discolouration is visible on the micromesh. **Right:** Picture of the micromesh taken with an electronic microscope. Mechanical damage around the rims of the holes can be observed. This leads to a severe deterioration of the detector gain and performance.

## 2. ANALYSIS AND RESULTS

### 2.1 Raw data analysis

The raw data from each detector are analysed by means of a pulse recognition routine that determines the amplitude and position in time of the detected signals, among other quantities. The signal baseline is determined by analysing the pre-trigger and post-acquisition window data, accounting for possible signals ( $\alpha$  or spontaneous fission) that may be present. Since the Pu samples are in the same chamber as the  $^{235}\text{U}$  it can be assumed that they receive the same neutron flux, while the fission count rates are sufficiently low to ignore pile-up effects.

### 2.2 The high neutron energy region

The interactions of the proton beam with the spallation target lead to a significant production of prompt  $\gamma$ -rays that reach the experimental area at the speed of light and constitute the bulk of what is commonly termed the “ $\gamma$ -flash”. In Micromegas detectors, this causes an initial signal lasting a few hundred ns, followed by a baseline oscillation that lasts for several  $\mu\text{s}$  or, in terms of neutron energy, down to 1-2 MeV. This behaviour can be clearly observed in Fig. 2 (top panel).

This problem can be mitigated by applying a software “compensation” technique [9] to the digitally recorded data. This method is based on the observation that the oscillations recorded in adjacent detectors for the same proton bunch are almost identical, as can be seen in Fig. 2 (top panel). The subtraction of the output of adjacent detectors causes the oscillations to largely cancel out, leaving a residual signal that consists primarily of signals attributable either to fission fragments or  $\alpha$ -particles (Fig. 2, bottom panel). This signal is then analysed with the peak search routine used for the lower energy region, thus extracting the desired pulse height spectra. The small residual of electronic noise is generally well below the amplitude threshold for fission fragment detection.

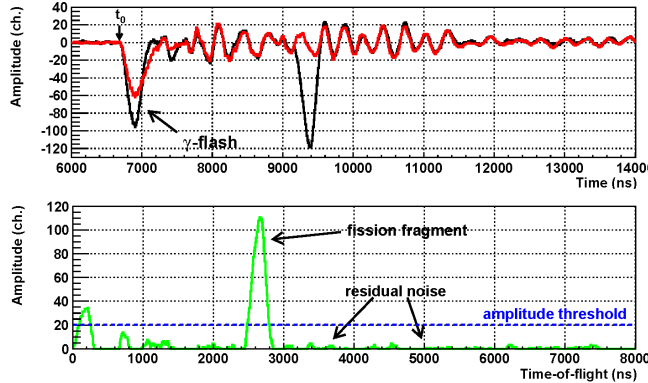


**Figure 2:** **Top:** The first few  $\mu$ s of the recorded signals during the same proton bunch from two adjacent detectors. The  $\gamma$ -flash signal and the baseline oscillations are clearly visible. **Bottom:** the residual signal after the subtraction of the two signals above. The oscillation is almost entirely suppressed.

### 2.3 Monte-Carlo simulations

The behaviour of the detectors was studied by means of Monte Carlo simulations performed with the FLUKA code [10,11], focusing particularly on the reproduction of the pulse height spectra of  $\alpha$ -particles and fission fragments for the evaluation of the detector efficiency and the quality of the peak-search routine. In Fig. 3, an experimental pulse height spectrum obtained from  $^{235}\text{U}$  and a simulated fission fragment spectrum can be compared.

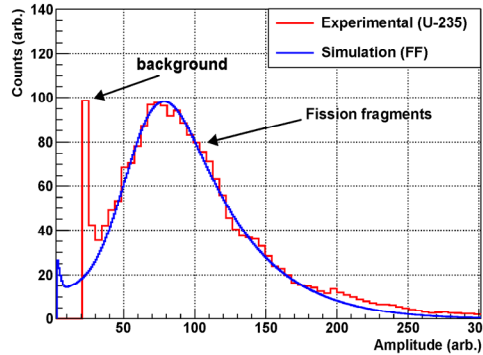


**Figure 3:** Experimental (red) and simulated (blue) pulse height spectra for  $^{235}\text{U}$ . The cut-off of the low-amplitude signals is due to the threshold set in the peak-search routine.

### 2.4 Results

The spontaneous fission background dominates the low energy region and remains important up to about 10 keV. Still, several resonances can be observed above this background. The first  $^{242}\text{Pu}$  resonance at  $\sim 2.7$  eV can be seen in the top left panel of Fig. 4, after subtraction of the spontaneous fission background, as determined with a fit of the beam-off data. The top right and bottom left panels show resolved resonances in the 700-800 eV region and up to approximately 28 keV, including a few not present in the evaluated libraries and, at a preliminary analysis, not attributable to any of the stated sample impurities. Data above 100 keV are shown in the bottom right panel of Fig. 4.

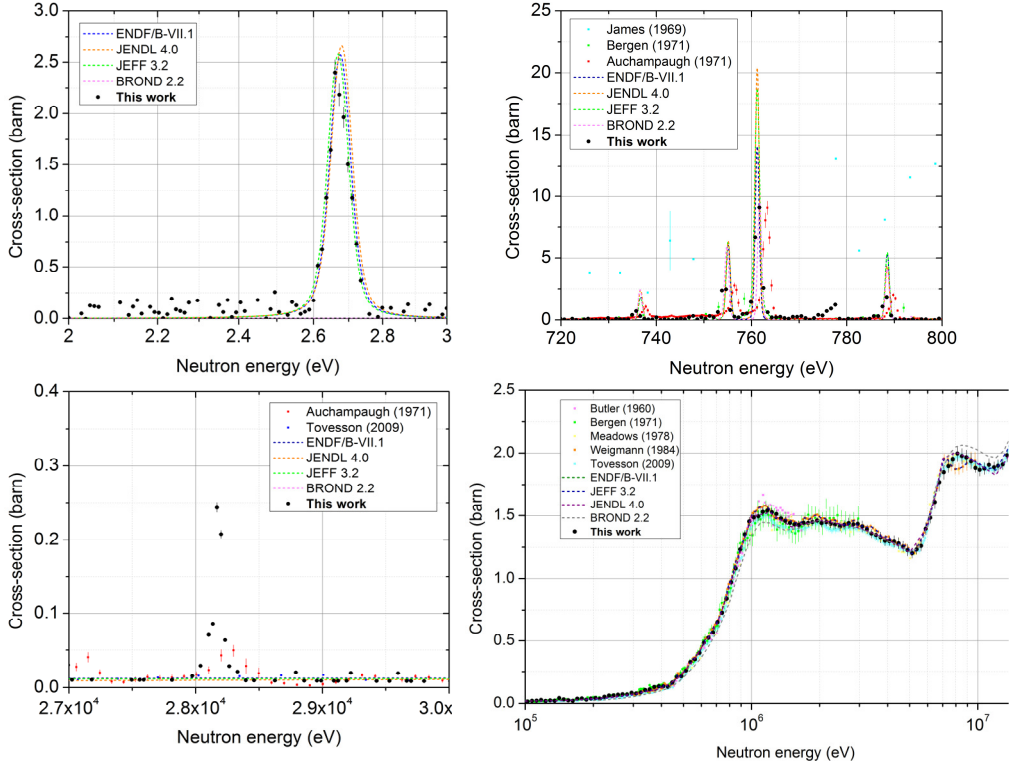


**Figure 4:** Selected resonances detected in the  $^{242}\text{Pu}(n,\text{f})$  data and data above the fission threshold, along with evaluated cross-sections from the ENDF/B-VII.1, JEFF 3.2, JENDL 4.0 and BROND 2.2 libraries: **Top left:** The first resonance at about 2.7 eV, **Top right:** several resonances between 730 and 790 eV, including one not previously detected at about 778 eV, **Bottom left:** the resonance at 28.2 keV. **Bottom right:** Data above the fission threshold.

### 3. THEORETICAL CALCULATIONS

A theoretical calculation of the  $^{242}\text{Pu}(n,\text{f})$  cross-section was performed with the EMPIRE nuclear reaction model code [12] (version 3.1). The level densities of the nuclei involved in the calculations were treated within the framework of the Enhanced Generalised Superfluid Model (EGSM). Initial values for the fission barrier parameters (barrier height and width) were retrieved from the RIPL-3 library [13] and subsequently adjusted to better reproduce the experimental data. Preliminary results can be seen in Fig. 5.

### CONCLUSIONS

Preliminary results from the  $^{242}\text{Pu}(n,\text{f})$  experiment performed at the CERN n\_TOF facility are presented, along with theoretical calculations performed with the EMPIRE code. The experimental setup and analysis method is described, including auxiliary Monte-Carlo simulations and an off-line technique to recover high-neutron energy data affected by the prompt  $\gamma$ -flash.

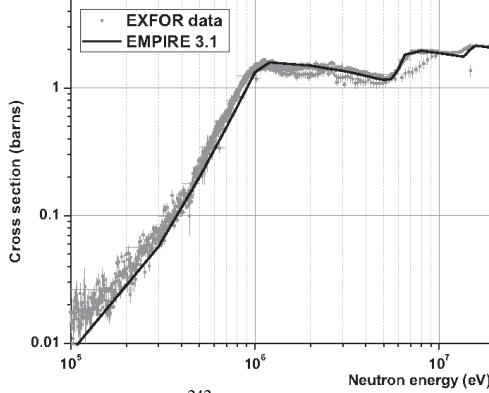


**Figure 5:** Theoretical calculation of the  $^{242}\text{Pu}(n,\text{f})$  cross-section performed with the EMPIRE code, with experimental data retrieved from the EXFOR database.

Analysis of the  $^{242}\text{Pu}(n,\text{f})$  data was complicated by the gradual detector gain shift. Among the issues that were addressed are the exact determination of the detector efficiency and the amplitude threshold correction, the accurate subtraction of the spontaneous fission background and the estimation of all uncertainties involved.

The energy range of interest was between 0.2-20 MeV, which is the range defined in the NEA Nuclear Data High Priority Request List. Nevertheless, several resonances were detected, ranging from 2.7 eV to 28.2 keV. The results above the fission threshold show general good agreement with respect to the most comprehensive and reliable past measurements, although differences of a few percent are found.

Finally, a significant part of the  $^{240}\text{Pu}(n,\text{f})$  was discarded due to the damage suffered by the detectors, as explained in section 1.4. Even under normal detector operation, the high  $\alpha$ -pileup probability (>30%) produces a long tail in the amplitude spectra that adversely affects the  $\alpha$ -fission fragment separation. A new experiment at n\_TOF new Experimental Area II should address these difficulties.

## REFERENCES

- [1] NEA Nuclear Data High Priority Request List, [www.nea.fr/html/dbdata/hprl/](http://www.nea.fr/html/dbdata/hprl/)
- [2] U. Abbondanno, Tech. Rep. CERN-SL-2002-053 ECT, CERN, Geneva (2002)
- [3] C. Guerrero et al., Eur. Phys. J. A **49**, 1 (2013)
- [4] E. Berthoumieux, [cds.cern.ch/record/1514680?ln=en](http://cds.cern.ch/record/1514680?ln=en)
- [5] G. Sibbens et al., J. Radioanal. Nucl. Chem. (2013) dx.doi.org/10.1007/s10967-013-2668-7
- [6] Y. Giomataris et al., Nucl. Instrum. Meth. A **376**, 29 (1996)
- [7] A. Tsinganis et al., CERN-INTC-2014-051. CERN, Geneva (2014), [cds.cern.ch/record/1706708](http://cds.cern.ch/record/1706708)
- [8] E. Chiaveri and the n\_TOF Collaboration, CERN-INTC-2012-029. CERN, Geneva (2012), [cds.cern.ch/record/1411635](http://cds.cern.ch/record/1411635)
- [9] N. Colonna et al., *A software compensation technique for fission measurements at spallation neutron sources*, Under preparation
- [10] A. Ferrari et al., Tech. Rep. CERN 2005-10, INFN/TC\_05/11, SLAC-R-773 (2005)
- [11] G. Battistoni et al., AIP Conf. Proc. **896**, 31 (2007)
- [12] M. Herman et al., Nucl. Data Sheets **108**, 2655 (2007)
- [13] R. Capote et al., Nucl. Data Sheets **110**, 3107-3214 (2009)